Journal of Fusion Energy, Vol. 9, No. 4, 1990

Measurement of Neutron Emission from Ti and Pd in Pressurized D_2 Gas and D_2O Electrolysis Cells

H. O. Menlove,[1] M. M. Fowler,[1] E. Garcia,[1] M. C. Miller,[1] M. A. Paciotti, R. R. Ryan,[1] and S. E. Jones[2]

Experiments using high-efficiency neutron detectors have detected neutron emission from various forms of Pd and Ti metal in pressurized D_2 gas cells and D_2O electrolysis cells. Four independent neutron detectors based on ^3He gas tubes were used. Both random neutrons (0.05–0.2 n/s) and time-correlated neutron bursts (10–280 n) of $\leq$100-μs duration were measured using time-correlation counting techniques. The majority of the neutron burst events occurred at $\sim -30°C$ as the samples were warming up from the liquid nitrogen temperature.

1. INTRODUCTION

The recent announcement by Flesichmann *et al.*,[1] that, excess heat and substantial neutron flux had been observed in Pd cathodes in electrochemical cells, stimulated numerous experiments, although several claims (for example, gamma rays from neutron capture) have been retracted.[2] Independently, Jones *et al*[3] observed 2.5-MeV neutron production at low levels during electrolytic infusion of D_2 into Ti and Pd electrodes, and discussed other means of creating non-equilibrium conditions, which might lead to "cold fusion." A replication of the latter experiment in the Gran Sasso Laboratory in Italy[4] provided confirmatory evidence for low-level 2.5-MeV neutron production. In addition, neutron emission has been reported in Ti subjected to pressurized D_2 gas and temperature changes.[5,6] We have measured neutron emissions at low levels in both electrolytic cells and in metals subjected to pressurized gases. In particular, we have observed the production of up to 300 n in bursts of $\leq$100-μs duration, as well as random or single neutron emissions.

We have measured both burst neutrons and random neutron emissions from a variety of sample types. The samples included cylinders of pressurized D_2 gas mixed with various forms of Pd and Ti metal chips, sponge, crystals, and powder. In addition, we have performed neutron measurements for electrolysis cells containing D_2O and cathodes of Ti, Pd, and V.

We are using four separate neutron detector systems operated in parallel experiments. The detectors all utilize ^3He gas proportional counters embedded in a polyethylene (CH_2) moderator. Three of the detectors are of the cavity- (well-) type, and one has an open channel for larger samples. The electronics are based on shift-register circuits[7] that give both the random and time-correlated neutron counting rates.

2. DETECTORS

Four similar detector systems were used in the present experiments to increase sample throughput and to

[1] Los Alamos National Laboratory, Los Almos, New Mexico 87545.
[2] Brigham Young University, Provo, Utah 84602.

0164-0313/90/1200-0495$06.00/0

act as control experiments. All of the detectors were located in the same underground experimental laboratory with separation distances of 1–2 m. There was negligible crosstalk between the detectors because of the small yield of the neutrons and the large solid-angle coupling of each sample to its primary detector. The characteristics of the four neutron detectors are listed in Table 1. The efficiencies were measured with a calibrated ^{252}Cf source (Av energy = 2.3 MeV). These compact high-efficiency detectors were developed at Los Alamos National Laboratory as part of the nuclear safeguards program, and detailed descriptions of the detectors can be found in Refs. 8–10. These detectors are well suited for detecting the neutron burst emissions for the following reasons:

- The neutron slowing and diffusion time jitter in the CH_2 gives an instantaneous burst of neutrons a time spread of ~40–50 μs (neutron die-away time in the detector related to neutron moderation, leakage, and capture).
- Four amplifier channels are used in each detector with electronic clipping time constants of ~180 ns.
- There is a de-randomizing buffer storage[7] at the input to the shift-register electronics to reduce deadtime for burst events.
- All neutron counts trigger the time correlation circuit without waiting through the gate time, thus reducing deadtime.
- High efficiency is required to detect a significant fraction of the small neutron bursts. The capability for time-correlated counting improves with the square of the neutron detection efficiency.

The ^3He detector tubes for Systems 1, 3, and 4 are screwed directly into an aluminum metal cavity that is sealed to prevent RF noise penetration, and desiccant is added to keep moisture out of the detector high-voltage area and to prevent any moisture from the test cells from affecting the counting system. Four AMPTEK A-III hybrid charge-sensitive pre-amplifier/discriminators[8] are located inside this sealed cavity. They are placed at the base of the ^3He counters to eliminate analogue signal transmission lines that are prone to pick up noise.

Time-correlated neutron counting[7] is essential for the neutron burst results reported in this paper. Every neutron count that enters the circuitry triggers the time-correlation counters that check whether there are any other neutron counts within the selected time gate. We use a coincidence time gate of 128 μs, which corresponds to about three times the neutron die-away time of the detector.

The time-correlated (coincidence) count R is related to the number of neutrons; (N) that are counted in the gate by the relationship

$$R = \frac{N(N-1)}{2}$$

Thus, if 100 n are emitted from the sample in a burst of <100 μs, our System 3 would detect ~34 n and R would equal 561. For our larger bursts, we have observed N from the increment in our totals (singles) scaler, and the calculated R using the above equation has agreed with the observed R in the coincidence scaler. If the burst event lasts more than 128 μs, N will be underestimated. The accidental coincidence counts are measured by sampling the shift registers after a delay of 1 ms following each neutron pulse.

Table I. Neutron Detector Characteristics

Identification	Shape[a]	Size	Number ^3He tubes	^3He pressure (atm)	Cavity size (cm)	Total efficiency (%)[c]	Bkg (s^{-1})	Coincidence Bkg (h^{-1})	Sensitivity limit (n/s)[c]
System 1	Rectangular	25 × 35 × 35 cm^3 channel	18	4	12 × 23 × 35	21	0.26	1.7	0.043
System 2	Cylindrical	23 cm ϕ × 37 cm cavity	6	4	5(diam) × 20	26	0.10	0.4	0.022
System 3	Cylindrical	22 cm ϕ × 35 cm cavity	16	6	9(diam) × 28	34	0.25	2.1	0.026
System 4	Cylindrical	22 cm ϕ × 35 cm cavity	16	4	9(diam) × 28	31	0.39	2.2	0.036

[a] System 2 has a single ring of ^3He tubes, whereas Systems 3 and 4 have double rings of ^3He tubes.
[b] The total efficiency was measured using a calibrated ^{252}Cf source located at the sample position.
[c] Sensitivity limit corresponds to the source random emission rate for an 8-h count (3σ above background). For the burst-type events, the sensitivity is about two orders of magnitude better.

Acoustical emission has been used for qualitative monitoring of cracking in the Ti samples. The sensor is a Dunegan/Endevdo acoustic transducer (Model D9203A-AD63) that is tuned to 150 kHz frequency and is attached to the outside of the sample bottle.

3. DATA SURETY

For low-level neutron counting and especially neutron burst counting, it is necessary to distinguish true neutron counts from spurious background noise. We have taken the following measures to assure that our burst events originate from neutrons:

- We use four separate detectors operating in parallel to pick up common sources of noise such as line voltage spikes, RF interference, cosmic-ray showers, and external room neutrons.
- We alternate dummy sample runs with the active sample runs.
- For System 3, we split the signal output to long (128-μs) and short (16-μs) gates and require that the gate count ratio be consistent with the detector die-away time (~50 μs).
- We collect singles counts, coincidence counts, and accidental counts and require that the three rates be consistent with observed neutron bursts.
- We detected the neutron bursts at a predictable time (2000–4000 s into the warm-up from liquid nitrogen, LN) and temperature (~ −30°C) for our first 12 bursts (samples Ti - 1 and Ti - 6) and many subsequent bursts.
- For sample numbers greater than Ti-17 we have added to System 3 a bank of Cd-covered ^{3}He tubes that measure only electrical noise and not neutrons. This acts as a veto for spurious electronic noise events. System 4 was upgraded with an external ring of eight ^{3}He tubes to monitor the inside/outside tube ratio to check for consistency with sample neutrons as compared to external source neutrons or electrical noise.

For System 3, we calibrated the gate fraction for instantaneous neutron bursts (spontaneous fission) using a ^{252}Cf source for which the ratio was 128-μs gate/16-μs gate = 3.18 ± 0.01. For the sum of several weeks of data collection in System 3, the long to short gate ratio was 3.2 ± 0.3 for the cosmic-ray background and 2.5 ± 0.4 for the sample neutron bursts. These ratios both agree statistically with the ^{252}Cf ratio and give additional evidence that the observed bursts are from neutrons. Cosmic-ray spallations give a source of instantaneous coincidence background neutrons, and the gate ratio was measured to be the same as a ^{252}Cf spontaneous-fission source.

Prior to the work reported in this paper, we operated detector System 1 and System 3 for 4 weeks measuring Pons-type[1] electrolysis cells. During these experiments, we observed no neutron bursts or excess random neutron emissions. In retrospect, these samples could be considered dummy samples.

Additional measurements were performed to ensure that environmental noise was not getting into the detector systems. The results of these tests were as follows: (1) no gamma-ray sensitivity up to 1 R/h, (2) the entire detector was cooled to −40° C with no change in performance, (3) no electrical noise pickup for noise generators (Telsa coils) placed directly into the detector cavity, (4) a long-term efficiency stability (precision) of 0.01%, and (5) no microphonic noise pickup for mechanical fracturing experiments or tests involving ultrasound in the detector cavity.

4. NEUTRON BACKGROUNDS

We performed four experiments to establish the source of our backgrounds: (1) we removed the CH_2 moderator from detector Systems 3 and 4 and covered the ^{3}He tubes with 0.4-mm-thick cadmium sheet; (2) for the normal detector configuration (System 3), we increased the sample mass (steel) six-fold and measured the increase in background; (3) we removed the neutron shielding from System 4 and measured the background rate at ground level; and (4) for System 2, we replaced the AMPTEK amplifiers with a conventional pre-amplifier plus multichannel analyzer to collect the 765-keV pulse-height spectrum from neutron capture in ^{3}He gas tubes.

4.1. Time-Correlated Counts

Our primary neutron burst results correspond to time-correlated counts. The time-correlated background counts are essentially all from cosmic-ray spallation neutrons originating in the detector body (CH_2 + Al) and the sample (steel + Ti). This was established by experiment number 1, for which the neutron efficiency is so small that the coincidence efficiency is negligible. For this experiment, the time-correlated counts were less than one per day.

For experiment number 2, the time-correlated background counts were 6.0 counts/h (6.5-kg steel bar), 2.3

counts/h (1.0-kg steel plus Ti sample), and 1.7 counts/h (empty counter).

For experiment 3 (no shielding), our average *time-correlated* background rate was 150 counts per hour compared with 1.7 counts/h in the shielded laboratory.

4.2. Uncorrelated (Random) Neutron Counts

Our uncorrelated background counts came from cosmic rays, uranium in our concrete shield, and α and β decay in the Al walls of our ^{3}He gas tubes.

Experiment number 4 showed that the integral count from the AMPTEK amplifier was about 50% larger than the counts in the 765-keV neutron peak distribution.

The random neutron background rates (count/s) in System 3 for experiment number 2 were 0.2495 ± 0.0011 (6.5-kg steel bar), 0.2455 ± 0.0006 (1.0 kg stainless steel plus 80 g Ti sample), and 0.2455 ± 0.0020 (empty counter). Thus, for counting times of several days, we cannot detect the presence of our normal sample as compared with an empty counter in our random neutron counting rate.

In summary, the key result was that removing all thermal-neutron counts (experiment 1) removed *all* time-correlated counts. The random neutron background from the α and β decay in the tube walls is constant and obeys normal random counting statistics for radioactive decay. Thus, long counting intervals can be used to establish this background baseline. The detectors are covered with approximately 15 cm of CH_2 shielding, and the background baseline is not significantly perturbed by the proximity of other objects in the room.

4.3. Background Fluctuations

The fluctuations in neutron background come from both the statistical component and the systematic component. The random statistical component is estimated by the square root of the counts. The systematic component comes from electronic drifts, external neutron sources, cosmic-ray variations, etc.

We performed a set of experiments to estimate the size of the two components. For the first experiment, we counted a high-rate (200,000 counts/s) fixed-neutron source (AmLi) in System 3 for a period of 4 weeks. The observed scatter (standard deviation) of the 10^4-s data points about the mean was only ±0.004%. Thus, the electronic drifts are less than this value.

For System 4, we measured the dummy sample background for 3 weeks. Each run was 10^4 s and we measured 184 runs. The mean value was 0.3924 counts/s and the observed standard deviation (scatter) was 0.0061 counts/s. The statistical standard deviation (RSD) from the square root of the counts was the same at 0.0062 counts/s.

For System 3, running the same type of experiment for 2 weeks yielded an average totals rate of 0.2455 counts/s with an observed standard deviation of 0.0048 count/s. The RSD for each 10^4-s counting period was 0.0049 counts/s, so the systematic fluctuations were negligible.

5. EXPERIMENTAL PROCEDURES

5.1. Pressurized D_2 Experiments

The Ti and Pd samples used in the D_2-gas-type experiments were contained in a pressurized stainless-steel gas cylinder with a volume of 250 cm^3 and an empty weight of 1 kg. After evacuating the sample for about 1 h at 150–200°C, the cylinder was backfilled with D_2 gas at room temperature and sealed. Some samples were flushed while hot with hydrogen or deuterium to partially remove the oxide layer. Additional surfaces free of oxide are created by the cracking of Ti during the temperature cycling. The amount of deuterium uptake was determined by measuring the pressure drop in the gas and by measuring the acoustical emissions from the hydride cracking in the Ti chips. We have measured a direct correlation between the acoustical emissions and the D_2 pressure drop. The expansion of the lattice volume by the absorption of deuterium causes additional stress and cracking during subsequent LN temperature cycles.

The sealed sample was put through multiple LN temperature cycles. Typically, the LN cooling would last for 20–60 min. The sample was then removed from the LN and placed in the neutron detector cavity and allowed to warm to room temperature.

The measurement time bins were typically 1000 s or 2000 s; however, longer time intervals were used for some of the overnight runs. A complete temperature cycle would take about 1 day for most cases. A few cycles were shorter, lasting ~5 h. Each cylinder was put through 7–23 temperature cycles. Several of the samples were counted during the cooling down phase of the LN cycle with negative results.

At this early phase of the investigations, we have focused on experiments that contained a wide variety of material forms to maximize the chance of getting a neutron yield. The samples that gave neutron emissions contained mixtures of Ti and Pd turnings, sponge, foils, crystals, and powders. At least some of the material had

Table II. Sample Materials

Sample identification	Gas	Pressure (psi) start-final[a]	Materials[b]
Ti-1	D_2	600-UN	111 g Ti sponge (2 g Ti crystals); 4.2 g Ti (6,6,2) chips
Ti-2	D_2	290-UN	~30 g Ti turnings (high temperature load)
Ti-3	D_2	290-UN	25 g Ti turnings (D_2 loaded at LN temperature)
Ti-4	D_2	400-UN	100 g Ti crystals, 100 g Ti sponge
Ti-5	D_2	600-UN	46.4 g Ti metal turnings
Ti-6	D_2	600-200	147 g Ti pieces, 17.4 g Ti powder, 4.6 g Pd powder, (D_2O electrolysis—22.8 g Ti sponge, 1.7 g Pd pieces)
Ti-7	D_2	580-14	33.3 g Ti sponge deuterided to ~Ti $D_{0.18}$
Ti-8	D_2	580-14	50 g Ti turnings, 4 g Ti sponge (D_2O elect.)
Ti-9	D_2	580-560	30 g Ti turnings and sponge (D_2O elect.)
Ti-10	D_2	580-UN	23 g Ti turnings, ~75 g Ti sponge ~4 g Ti crystals, 2 g Pd foils (all from D_2O elect.)
Ti-11	D_2	580-UN	82 g Ti powder, 10 g (90% Ti + 10% Pd) sintered powder
DH-1	$D_2 + H_2$	(425 + 425) − 842	30 g Ti alloy (6,6,2)[a] chips
DD-2	D_2	150-0	10 g Ti (6,6,2), 68 g Ti (6,4) chips
DD-3	D_2	830-816	10 g Ti (6,6,2), 68 g Ti (6,4) chips (deuterided during loading)
Ti-12	D_2	580-UN	14.8 g Ti sponge (D_2O elect.)
Ti-13	D_2	580-UN	10.3 g Ti (6,6,2) chips
Ti-14	D_2	550-UN	60 g Ti (6,6,2) chips
Ti-15	D_2	550-UN	50 g Ti sponge, 20 g Ti (6,6,2) chips
Ti-16	D_2	150-14 {520-100, 500-150} refill	30 g Ti sponge, 34 g Ti-Pd-sintered powder, 45 g misc./ cathodes of Pd, Ti, Ni, Zr, V
Ti-17	D_2	40-14	60 g Ti (6,6,2) chips
DH-4	$H_2 + D_2$	196-0	80 g Ti (6,6,2) chips (deuterided during loading)
DD-5	D_2	40-0 (400-UN) refill	50 g Ti (6,6,2) chips
Ti-18	D_2	520-460	60 g Ti (2,3) chips

been used in electrolysis experiments of the Jones type.[3] Forty-two gas cylinder samples have been used in the experiments and 14 have yielded neutron emissions. Our attempts to run experiments using a single material component to isolate the neutron source have had limited success because of the intermittency of the effect. That is, the "right material" might still give a negative result because of variations in surface condition or some other feature required for the emission of neutrons. (Table II gives a listing of the contents of the gas samples measured through September 1989).

Three dummy samples (filled with air and Ti) and five H_2 gas cylinders were used for control runs. The stainless-steel gas cylinders were the same size and mass as for the normal samples. The Ti masses ranged from 50–200 g for the control cylinders. For many control runs, the same steel cylinder would be used for repeat experiments where the Ti was changed. Also, for the normal samples, the same steel cylinders were used for multiple samples where the Ti and gas fills were changed. Details on the H_2 gas control cylinders are given in Table II.

5.2. D_2O Electrolysis Experiments

In addition to the gas phase experiments, we have run four experiments using Jones-type[3] cells and electrolytes. Each of the experiments had six D_2O cells located in System 1. The anodes were gold foils and the cathodes were Ti, Pd, V, and Zr (foils, crystals, sponge, and sintered powder).

For one experiment, the electrolyte was D_2O mixed with the multiple ingredients described in Ref. 3. For the other three experiments, the electrolyte was an acidified (pH = 4) 10-g/L Li_2SO_4/D_2O solution. The currents and voltages were varied over the range from 0–4 A and 0–16 V, respectively. Sometimes the voltage was pulsed (700 ms on, 100 ms off). The data were collected in 1000-s or 2000-s time bins, and the experiments lasted for several

Table II. Continued

Sample identification	Gas	Pressure (psi) start-final[a]	Materials[b]
Ti-19	D_2	520-500	36 g Ti (6,4) chips
Ti-20	D_2	500-UN	50 g Ti (6,6,2) chips
Ti-21	D_2	480-400	45 g Ti-Pd (80:20) sintered powder, 63 g Ti sponge cathodes, 5 g V and Zr foil
Ti-22	$H_2 + D_2$	500-300	50 g Ti (6,4) and 50 g Ti (6,2) chips
Ti-23	D_2	480-UN	50 g Ti (6,6,2) chips
Ti-24	D_2	480-UN	50 g Ti (6,4) chips
Ti-25	D_2	460-14	50 g Ti (10,3,2) chips
Ti-26	$H_2 + D_2$	(240 + 460) - UN	133 g Ti (6,4) chips
Ti-28	$H_2 + D_2$	(250 + 250) - 30	50 g Ti (6,6,2), 33 g Ti (6,4) chips
Ti-30	D_2	460-0	100 g Ti sponge
Ti-31A	D_2	750-300	50 g Ti (6,6,2), 50 g Ti (6,4) chips
Ti-32	D_2	750-110	100 g Ti (6,6,2) chips
Ti-33	D_2	750-600	100 g Ti (6,4) chips
Ti-34	D_2	750-0	32 g Ti (6,6,2) elect. cathodes
Ti-36	D_2	750-580	21 g misc. Ti, Zr, V cathodes
Pd-1s	D_2	1000-1000	20 g Pd deuterided metal
Pd-3s	D_2	1000-1000	20 g Pd deuterided metal
Pd-4s	D_2	1000-1000	20 g Pd deuterided metal
Pd-5L	D_2	1000-1000	800 g Pd deuterided metal
H_2 gas controls			
Pd-H2	H_2	1000-1000	20 g Pd metal (hydrided)
Ti-27	H_2	500-30	20 g (6,6,2), 20 g Ti (6,4), 20 g Ti (10,2,3)
Ti-29	H_2	500-40	50 g Ti (6,6,2), 50 g Ti (6,4) chips
Ti-31	H_2	680-480	50 g (6,6,2), 50 g Ti (6,4) chips
Ti-35	H_2	680-28	50 g Ti (6,6,2), 50 g Ti (6,4) chips
Electrolysis	Electrolyte	NA	$Cell_1$-V foils, $cell_2$-PdTi-sintered powder, $cell_3$-Zr foil, $cell_4$-Pd foil, $cell_5$-PdTi-sintered powder, $cell_6$-V foil. (D_2O/Li_2SO_4 electrolyte).
14B	D_2O/Li_2SO_4		

[a] The start pressure corresponds to the start of the counting period. UN represents an unknown pressure at the end of the measurements.
[b] Ti (6,6,2) is an alloy of Ti with 6% Al, 6% V, and 2% Sn by weight, and Ti (10,2,3) is an alloy of Ti with 10% V, and 2% Fe 3% Al, by weight.

days to a week. The controls were six D_2O cells of the same size and mass as the sample runs but without electrodes or six identical operating cells with H_2O replacing D_2O. The detectors gave the same background rate for the dummy sample and an empty sample cavity.

6. RESULTS

6.1. Gas Phase Experiments

6.1.1. Burst Results

The first burst-type neutron emissions were observed in April from the gas-filled cylinder Ti-1 as shown in Fig. 1a.

The next several cylinders were loaded with single Ti and Pd components in unsuccessful attempts to isolate the material that gave the neutron emissions. After four samples with null results, another multi-component cylinder was measured with burst yields as shown in Fig. 1b.

Both Ti-1 and Ti-6 demonstrated a pattern of bursting during the third or fourth 1000-s time interval during the warm-up. The frequency distribution for the bursts from samples Ti-1 and Ti-6 peaked at 2800 s into the warm-up cycle as shown in Fig. 2a.

To help establish the cylinder temperature vs. the warm-up time, the dummy cylinder was run through the LN cycle with a thermocouple temperature probe inside the cylinder at the general location of the Ti material. The most probable temperature for the neutron burst ob-

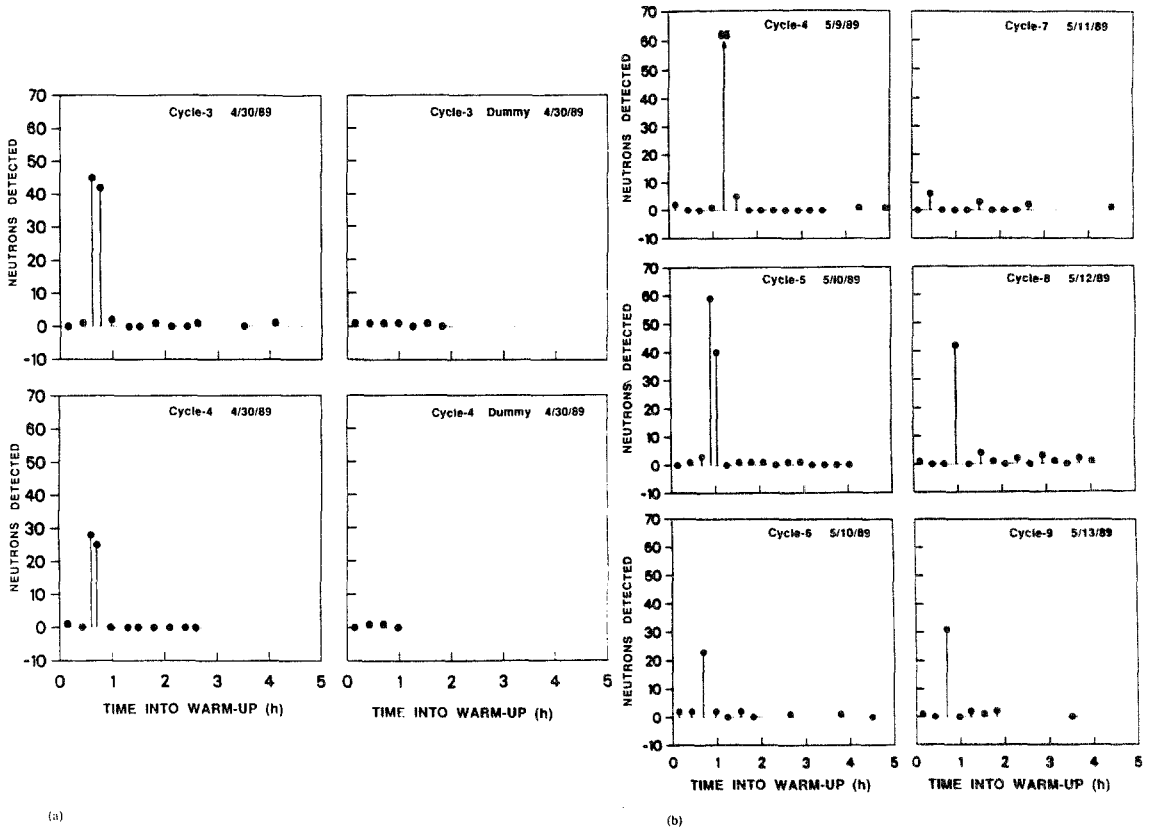

Fig. 1.(a) The combined coincidence results for the Ti-1 sample (left side) and the dummy cylinder (right side) that were measured in System 3. The dummy and the T-1 sample were measured alternating in time in the detector. Time zero represents the removal of the cylinder from the LN for both the sample and dummy. The ordinate corresponds to N, the number of neutrons detected in the 1000-s time bins. These neutron bursts were shown to arrive within a time of less than 100 μs. The average number of coincidence counts in the dummy runs was one count every 2000 s. The control counter (System 4) gave null results during the entire experiment. (b) The coincidence results, N, for six active cycles for sample Ti-6 measured in System 3. The neutron burst results mostly occur 2000–4000 s into the warm-up period. The ordinate N is the number of neutrons detected in individual bursts. The largest burst gave 85 neutron counts representing a source term of 253 n.

servations was approximately −30°C with a wide temperature distribution as shown in Fig. 2a.

The significance of the relationship between the temperature and the neutron bursts is yet to be established. It might be related to phase changes in the metal or to other stress conditions. If Ti metal is deuterided to a sufficiently high level, it has the possibility of going through a phase transition between 77–300°K. However, none of the samples that had been pre-deuterided at elevated temperatures gave neutron yields.

We also have observed bursts from a cylinder (DH-1) loaded with 30 atm of D_2 plus 30 atm of H_2 gas. The addition of the H_2 gas was motivated by the possibility of obtaining p + d fusion in future experiments and measuring the high-energy (5.4-MeV) gamma rays.

This sample gave no bursts during the warm-up from LN temperature; however, we have observed at least four neutron bursts from the cylinder at room temperature as shown in Fig. 3b.

We have recently run hydrogen gas control experiments with five samples loaded with H_2 gas in place of D_2 gas. There was no excess neutron yield from these five experiments over a period of several months. These cylinders are now serving as control cylinders for alternating runs with the sample cylinders. After 5 days of measuring the H_2 gas control sample Ti-31, the H_2 gas was replaced by D_2 gas and the sample was renamed Ti-31A. The refilled sample Ti-31A subsequently gave two large bursts during the warm-up from LN at ~ −30°C (see Table III).

6.1.2. Random Neutron Emissions

In addition to the burst-type results, we have measured random neutron emissions from several of the gas

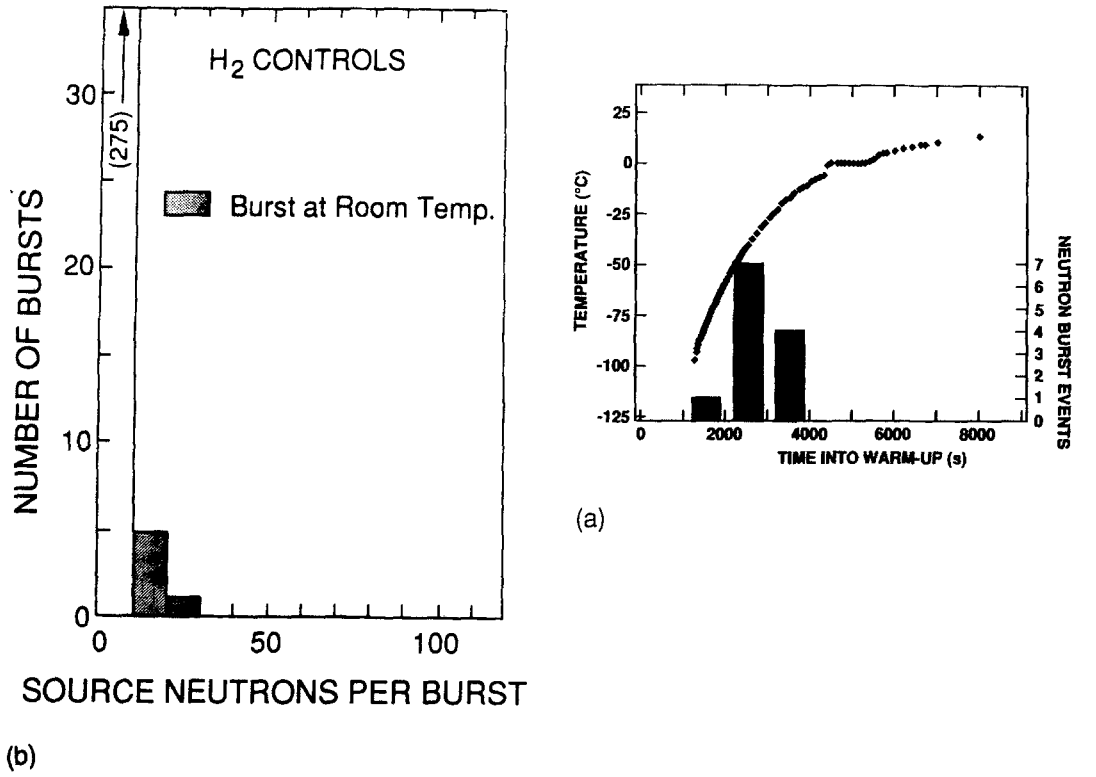

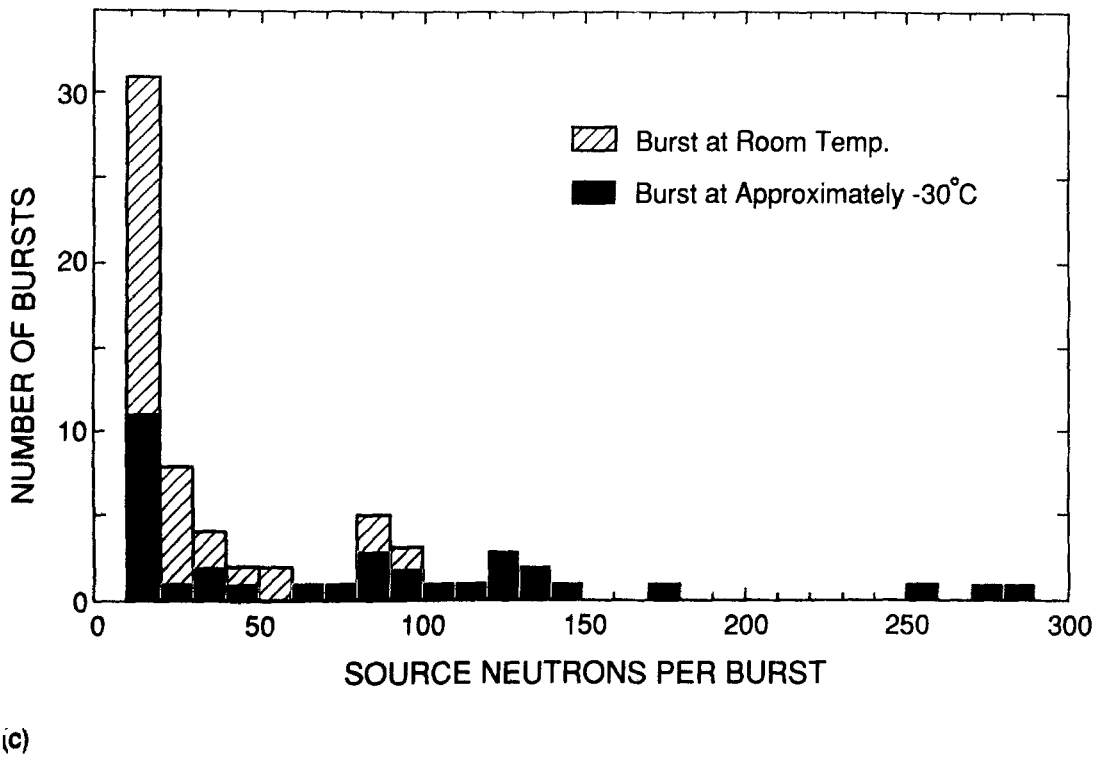

Fig. 2.(a) The number of neutron burst events vs. time and temperature into the LN warm-up cycle for samples Ti-1 and Ti-6. These 12 bursts represent all of the burst events from approximately 500 h of counting these two samples. (b) The number of neutron burst events vs. the number of source neutrons per burst for 1280 h of H_2 control sample measurements (see Table III). The low multiplicity events ($n<10$) dominate, and there are no events with high multiplicity ($n>20$) and no events ($n>10$) during the warm-up from LN temperature. (c) The number of neutron burst events vs. the number of source neutrons per burst for the active samples listed in Table III. The events with lower multiplicity are much more frequent than the high multiplicity events. The events emitting less than 10 n are buried in the cosmic-ray background spallations events. The darkened data correspond to events that occurred at the LN warm-up temperature between -100°C and 0°C.

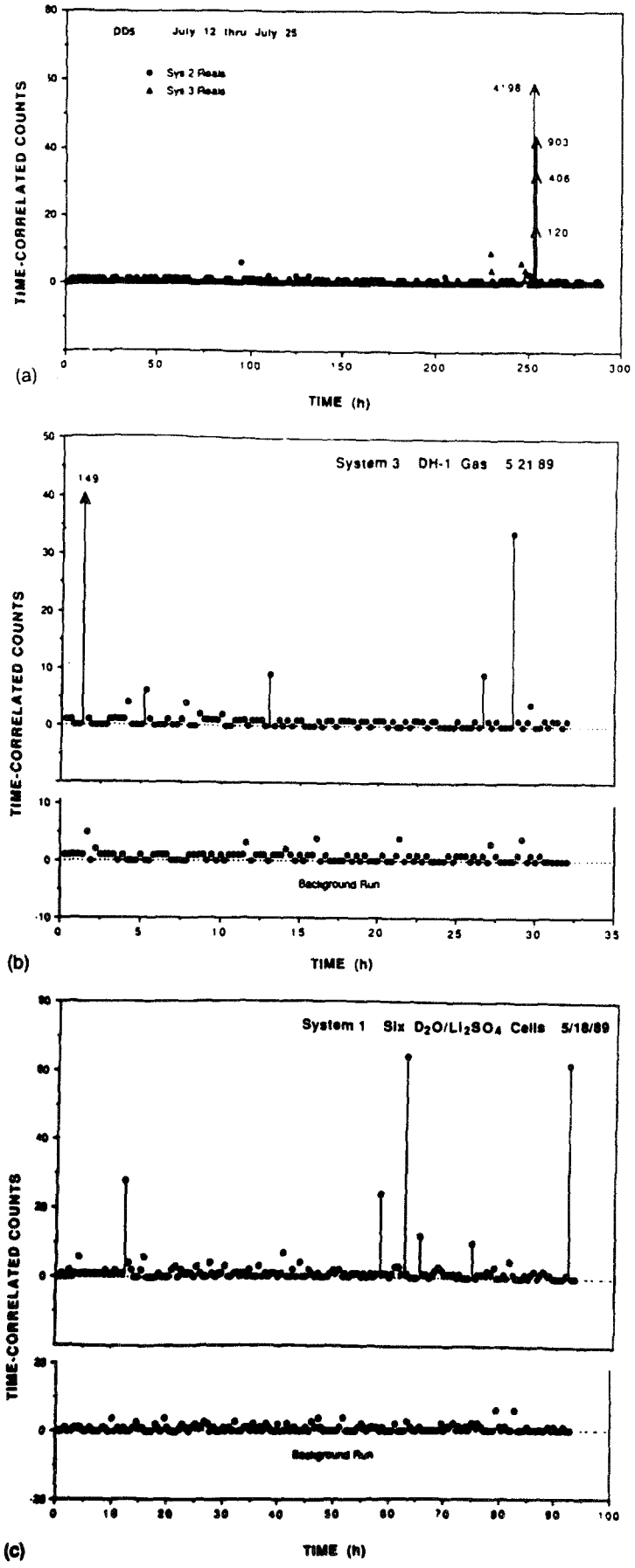

Fig. 3.(a) The number of coincidence counts R, in 2000-s time bins vs. measurement time for sample DH-5 measured in Systems 2 and 3. The large burst events at approximately 250 h occurred at a sample temperature between -100 and 0°C during the warm-up on LN cycle 6. (b) The number of coincidence counts R, vs. time for sample DH-1 (top curve) and the dummy cylinder (bottom curve). All of the bursts occurred at room temperature. The ordinate corresponds to the number of time correlated counts measured during the 2000-s time bins. The background coincidence counts result from cosmic-ray neutron bursts in the detector. The first sample burst occurred about 18 h after the first LN cycle. (c) The coincidence neutrons counts, R, vs. time for six D_2O electrolysis cells measured in System 1. The bottom data correspond to six D_2O dummy cells measured in the same detector immediately after the sample run was completed. The ordinate corresponds to the number of time-correlated counts R measured during the 2000-s time bins. The burst activity continued for several hours after cutting off the current at 71 h into the experiment. The control runs taken in Systems 3 and 4 gave no burst activity or change in background rates during either the sample run or the dummy runs. The largest burst corresponds to a source term of approximately 130 n.

Table III. Summary of Neutron Burst Results

Starting date (Mo/d/y)	Sample Number	Number of source Neutrons[a]	Burst cycle (time)[b]	Total time (h)[c]
Active samples				
4/28/89	Ti-1	**127, 136, 85, 76**	3(75), 3(75), 4(80), 4(80)	180
5/6/89	Ti-6	**258, 179, 121, 70, 15, 127, 94**	4(92), 5(110), 5(110), 6(116), 7(140), 8(164), 9(188)	336
5/19/89	DH-1	55, 15, 15, 27	1(48), 2(55), 2(72), 2(78)	264
6/2/89	DD-2	12, **85, 15, 15, 39, 142**, 18, 30	0(15), 0(25), 1(48), 1(49), 2(97), 2(97), 2(99), 3(123)	300
6/20/89	Ti-14	15, 91, **12, 24**	2(48), 2(72), 4(96), 5(120)	200
6/28/89	Ti-16	24, 24, 12, **15**, 18, 15, 15, **109, 18**	1(50), 2(72), 2(72), 3(96), 4(144), 5(145), 5(146), 7(150), 8(310)	420
7/7/89	DD-5	**12, 279, 130, 88, 48**	6(312), 6(312), 6(313), 6(313), 6(314)	620
7/18/89	Ti-19	**88**, 15	1(50), 6(216)	350
8/18/89	Ti-22	55, **97**	2(72), 3(98)	288
8/11/89	Ti-23	**19, 23, 19**	0(10), 1(82), 5(226)	260
8/8/89	Ti-24	35, **119, 16**, 16, 16, 15, 15	0(24), 2(144), 2(144), 3(168), 3(169), 3(171), 6(216)	316
8/29/89	Ti-30	**280, 13**	6(312), 8(408)	480
9/11/89	Ti-31A	**86, 34**	7(336), 7(336)	500
9/12/89	Ti-32	**23, 35**	1(2), 1(19)	380
Borderline samples				
5/16/89	Ti-10	**12, 15**	6(96), 7(122)	240
6/9/89	DH-4	**21**	2(120)	200
6/12/89	Ti-13	**24**	1(28)	140
8/22/89	Ti-25	**32**	3(72)	280
8/24/89	Ti-28	**17**	2(28)	250

Inactive samples (Ti)	Run h[c]	Pd samples	Run h[c]	H_2 controls	Run h[c]
				$Pd-H_2$	110
Ti-2	120	Pd-1s	110	Ti-27	220
Ti-3	100	Pd-3s	90	Ti-29	216
Ti-4	108	Pd-4s	120	Ti-31	62
Ti-5	91	Pd-5L	110	Ti-35	630
Ti-7	84				
Ti-8	120				
Ti-9	132				
Ti-11	168			SS + Ti	2600
DD-3	156				
Ti-12	260				
Ti-15	210				
Ti-17	280				
Ti-18	170				
Ti-20	260				
Ti-21	212				
Ti-26	330				
Ti-36	320				

[a] The **bolded source neuron** values corresponded to the burst occurring between −100°C and 0°C during warmup from LN temperature.
[b] The designation 3(75) represents a burst during cycle 3, 75 h after loading the D_2 gas.
[c] The time represents the total sample measurement time.

cylinders. The electronics that we are using were designed to separate purely random neutron emissions from time-correlated bursts in which two or more neutrons emitted at the same time are considered a correlated event.[8] The results for sample Ti-1 are shown in Fig. 4.

Immediately following the Ti-1 overnight run, in System 4 the sample (Ti-1) was counted alternating between Systems 3 and 4 with the dummy in the opposite detector. These runs were for 4000 s each with two round trips in each detector for a total of 8000 s in System 3 plus 8000 s in System 4. Sample Ti-1 gave an excess of random neutron counts in both systems with a significance level in System 3 of 2.6σ and 3.6σ in System 4. The combined (both detectors) significance for Ti-1 was 4.3σ above the dummy background baseline. No temperature cycling was involved during this period.

Sample Ti-3 gave an excess random neutron emission during the 5-h period following the first LN temperature cycle. The average totals rate was 0.2594 ± 0.0034 counts/s for the 5-h period, which was 4.3σ above the dummy background baseline rate of 0.2413 ± 0.0025 counts/s that was measured for a 11-h period before and after the sample run. The adjacent control detectors gave a constant background rate during the sample and background time periods. Subsequent temperature cycling of this sample gave no random or burst emissions.

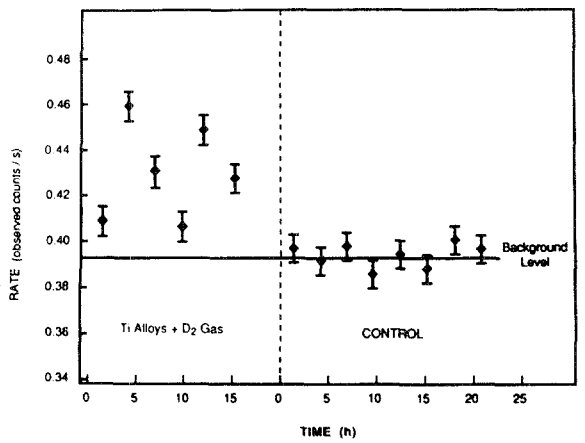

Fig. 4. The totals (random) neutron counting rate for sample Ti-1 measured in System 4 over a 17-h time period at room temperature after the first two LN cycles. The right-hand section of Fig. 3 corresponds to data for the dummy sample in System 4, and the time line is reset to zero when the dummy count starts. The data taken in the control counter (System 3) during the same two nights gave a constant background rate during the two nights. The average of the 17-h sample data was 0.4298 ± 0.0027 counts/s, whereas the average of 22 h of the dummy runs was 0.3943 ± 0.0022 events/s. The difference in the two average values corresponds to a 10.3σ significance level.

For the random neutron emission results, long counting intervals are required to statistically differentiate the low-level emission rates (0.05–0.2 n/s) from the background rate.

6.2. D_2O Electrolysis Results.

We performed three experiments with Jones-type[3] cells where each experiment involved six D_2O cells containing different cathodes of Ti, Pd, Zr, and V metal. While two experiments showed ~3σ results above background levels, the limited sensitivity in the random-counting mode precludes any definitive statement concerning neutron emission at this time.

A fourth experiment gave burst yields after running the current for about 12 h of electrolysis, and the bursts continued for several days as shown in Fig. 3c.

7. SUMMARY

We have observed both burst and random neutron emissions from 14 samples involved in 42 different experiments. Table III gives a summary of the results. Two different detector systems have been used to measure the random emissions and all four systems have detected the burst results. The individual burst results are as much as two orders of magnitude above the background levels.

Cosmic-ray neutron bursts are responsible for the coincidence background. Typical background counts are shown in Figs. 1,3, and 4 for the dummy runs. Some of the sample burst results could be large cosmic-ray bursts, but they should also be showing up during the background runs. The largest background burst that we have observed in the four systems over a 20-week period was 9 n detected (a source term of 30 n) in System 4. Samples Ti-1 and Ti-6 yielded neutron bursts at a predictable time into the experiment: all 12 neutron bursts occurred between 2000–4000 s into the LN warm-up cycle.

The results reported in this work do not define the neutron production mechanism. Several models have been proposed for the production of neutrons in the two types of experiments for which they have been detected; that is, electrochemical experiments and those in which various forms of Ti metals or alloys have been subjected to thermal cycling under D_2 gas at pressure. The possibility of particle acceleration caused by charge separation during a fracturing process has been suggested.[11–13] In support of the latter suggestion, both electron and positive

particle emission have been observed at energies of several keV on a time scale consistent with our observed neutron bursts during the mechanical fracture of $TiD_{0.8}$.[13] Fracturing and fatigue from hydriding of the samples have been observed after the samples were removed from the cylinders in most cases where neutron emission has been detected in our laboratory.

The random emission results *cannot* be explained as a large number of small bursts because sample Ti-1 gave approximately 2000 random neutron counts during the 17-h period with no net correlations (including neutron pairs) that were distinguishable above the cosmic-ray background. There are possibly different mechanisms responsible for the burst results and the random neutron emissions. The common denominator for all of the neutron emissions is that the samples are in non-equilibrium conditions because of temperature cycling and deuterium diffusion into or out of the samples.

Detailed characteristics of the materials that give the neutron emissions have not been established. It is difficult to isolate the material characteristics that are responsible for the neutron emissions because of the intermittency of the emissions. Bulk deuteration of the Ti and Pd has always given negative experimental results. The acoustical emissions were directly correlated with the hydriding and D_2 gas pressure decrease. Samples that had more cracking were more likely to yield neutron bursts. However, there were not acoustical emissions at the time of the measured neutron bursts. Two samples (DH-4 and DH-5) were deuterated to saturation inside the neutron detector, and even though tens of thousands of acoustical emissions were measured, no excess neutron yield was observed.

The frequency of large neutron-burst emission is very low, with an average rate of about 0.003 h^{-1} for bursts of 20 or more source neutrons. However, the majority of neutron bursts occur while the sample is in the -100–0°C range, although only about 4% of the measurement time involves this temperature range. The H_2 control samples have all been inactive.

Pressurized D_2 gas experiments similar to our work have been performed at Sandia National Laboratory[14] with negative results. However, their sensitivity for measuring coincidence neutron bursts was an order of magnitude less than for our experiments and their sample measurement times were shorter than ours.

We have yet to determine the neutron energies because the yields still are too low for the neutron spectrometry measurements. For the random emission yields, the levels (~0.08 n/s) were similar to the yields reported by Jones *et al.*[3]

Our future work will focus on the characterization of the material to obtain higher yields and to understand the neutron source mechanism. We will measure the neutron energy and repeat the experiments with HD and DT gas to help establish if the neutrons are originating from cold fusion,[15] hot fusion (during cracking and fractures), or some other source.

ACKNOWLEDGMENTS

The authors wish to acknowledge the useful discussions with M. P. Baker, G. W. Eccleston, P. A. Russo, and W. L. Bongianni during the early phases of these experiments. We are indebted to S. Taylor, J. Maxwell, and D. Mince for their assistance in sample preparation, and to H. R. Maltrud and J. M. Newmyer for help in controlling the deuteriding of Ti. We are grateful to E. Leonard for initiating the acoustical monitoring and to T. Feiertag for the use of his acoustical sensors. We are also grateful for the support of the Department of Energy, Division of Advanced Energy Projects for portions of this work. The use of high-efficiency neutron detectors with time-correlation circuitry developed under the support of the Department of Energy, Office of Safeguards and Security, was essential to obtain the results reported in this paper.

REFERENCES

1. M. Fleishmann, S. Pons, and M. Hawkins. (1989. *J. Electroanal. Chem.* **261**, 301–308.
2. M. Fleishmann *et al.* (1989). *Nature*, **339**, 667.
3. S. E. Jones *et al.* (1989). *Nature*, **338** (April 27), 737–740.
4. A. Bertin *et al.* (1989). *Nuovo Cimento*, **101A**, (June), 997–1004.
5. F. Scaramuzzi *et al.* (1989). Report from Frascati Research Center, April 18.
6. M. Yagi *et al.* (1989). *J. Radioanal. Nucl. Chem. Lett.*, **137**(6), 411–420.
7. J. E. Swansen, P. R. Collinsworth, and M. S. Krick (1980).Los Alamos Scientific Laboratory Report LA-8319-MS (April), *Nucl. Instr. Meth.*, **176**, 555.
8. H. O. Menlove and J. E. Swansen (1985). *Nucl. Technol*, **71** (November), 497–505.
9. H. O. Menlove, O. R. Holbrooks, and A. Ramalho (1982) Los Alamos National Laboratory Report LA-9544-M (ISPO-181), November.
10. H. O. Menlove (1981). Los Alamos National Laboratory Report LA-8939-MS (ISPO-142), August.
11. V. A. Klytuev *et al.* (1986). *Sov. Tech. Phys. Lett.*, **12**(11), 551–552.
12. J. S. Cohen and J. D. Davies (1989). *Nature*, **338** (April 29), 705–707.
13. J. T. Dickinson *et al.* Los Alamos National Laboratory Report (submitted).
14. J. E. Schirber *et al.* (1989). *Fusion Technol.* **16**, 397–400.
15. C. D. Van Siclen and S. E. Jones (1986). *J. Phys.* G **12**, 213–221.